Kallis, G. B., & Holmgren, A. (1980) J. Biol. Chem. 255, 10261-10265.
Katti, S. K., LeMaster, D. M., & Eklund, H. (1990) J. Mol. Biol. 212, 167-184.
Langsetmo, K., Sung, Y.-C., Fuchs, J., & Woodward, C. (1990) in Current Research in Protein Chemistry (Villafranca, J., Ed.) pp 449-456, Academic Press, New York.
Rance, M., Sørensen, O. W., Bodenhausen, G., Wagner, G., Ernst, R. R., & Wüthrich, K. (1983) Biochem. Biophys. Res. Commun. 117, 479-485.
Reutimann, H., Straub, B., Luisi, P. L., & Holmgren, A. (1981) J. Biol. Chem. 256, 6796-6803.

Electrophoretic and Hydrodynamic Properties of Duplex Ribonucleic Acid Molecules Transcribed in Vitro: Evidence That A-Tracts Do Not Generate Curvature in RNA†

Frank-Ulrich Gast and Paul J. Hagerman*

Department of Biochemistry, Biophysics, and Genetics, University of Colorado Health Sciences Center, Denver, Colorado 80262

Received November 20, 1990; Revised Manuscript Received January 30, 1991

ABSTRACT: We have developed a T7 RNA polymerase based transcription system for the production of fully complementary RNA molecules (i.e., molecules capable of forming blunt-ended duplex species) as the direct products of transcription, thus rendering unnecessary the enzymatic removal of single-stranded ends. A combined gel electrophoretic and hydrodynamic analysis of a 180 bp double-stranded (ds) RNA molecule containing four A_5-tracts in approximate phase coherence with the helix repeat provides no indication that the helix axis is curved, in sharp contrast to DNA molecules containing phased A-tracts. The electrophoretic behavior of dsRNA molecules reveals that their mobilities in nondenaturing acrylamide gels are approximately 10-20% lower than the corresponding mobilities of duplex DNA, in accord with earlier observations in the literature. Furthermore, the relative mobilities are only slightly modulated by gel concentration, the concentration of monovalent salt, or the presence of spermidine and/or Mg^{2+}. The reduced mobilities are not caused by increased contour length, since direct hydrodynamic measurements using transient electric birefringence indicate that the average helix rise, h, of the dsRNA molecules examined in the current study is 2.8 ± 0.1 Å/bp. The reduced electrophoretic mobilities, extrapolated to zero acrylamide concentration, are consistent with the lower residual charge predicted for dsRNA by counterion condensation theory. Finally, birefringence measurements indicate that dsRNA is only marginally stiffer than DNA, with a persistence length of ca. 500-700 Å.

A precise knowledge of RNA structure is important in many areas of molecular biology. For example, such knowledge is prerequisite to a detailed understanding of RNA-protein interactions (Wu & Uhlenbeck, 1987; Malim et al., 1990), RNA-catalyzed processes such as self-splicing of intervening-sequence RNA (Zaug & Cech, 1986; Murphy & Cech, 1989), the self-cleaving of plant satellite RNA (Uhlenbeck, 1987; Symons, 1989), and the processing of tRNAs by ribonuclease P (Guerrier-Takada et al., 1983, 1989), the mechanism of action of the ribonucleoprotein telomerases (Greider & Blackburn, 1989; Shippen-Lentz & Blackburn, 1990), and the mechanisms involved in protein biosynthesis (Moazed et al., 1986; Draper et al., 1988; Sampson et al., 1989; Denman et al., 1989).

An important advance in the study of RNA structure has come about through the development of preparative in vitro transcription systems, thus enabling the efficient production of RNA molecules of virtually any sequence and length for physical studies. One widely used technique is based on the use of RNA polymerase from bacteriophage T7. Plasmids bearing the T7 late promoter can be grown in *Escherichia coli* without interference from bacterial RNA production. Moreover, the T7 RNA polymerase can be overproduced in large amounts (Davanloo et al., 1984), thus facilitating the production in vitro of milligram amounts of RNA transcript. RNA molecules transcribed in vitro have been employed to address a number of issues regarding RNA structure, including the helix repeat of duplex RNA (Tang & Draper, 1990; Bhattacharyya et al., 1990), the conformations of internal loops (Varani et al., 1989), and the local conformation of a plant viroid self-cleaving domain (Heus et al., 1990). Principal methods for studying RNA structure have included either two-dimensional NMR (van den Hoogen et al., 1988; Chou et al., 1989; Puglisi et al., 1990) or chemical protection assays (Moazed et al., 1986; Ehresmann et al., 1987). However, while both approaches provide a detailed picture of local helix structure, they are not sensitive to longer range structure (e.g., branch geometries).

Two experimental approaches that have proven to be useful for the study of long-range structure in DNA should be directly applicable to the study of RNA structure. The first approach,

† This work was supported by grants from the National Institutes of Health, GM35305 (to P.J.H.), and the Deutsche Forschungsgemeinschaft, Ga351/1-1 (to F.-U.G.).

* Author to whom correspondence should be addressed at the Department of Biochemistry, Biophysics, and Genetics, University of Colorado Health Sciences Center, B-121, 4200 E. Ninth Ave., Denver, CO 80262.

0006-2960/91/0430-4268$02.50/0

polyacrylamide gel electrophoresis (PAGE),[1] has been used extensively to characterize the curvature of DNA molecules containing phased tracts of A residues [Wu & Crothers, 1984; Hagerman, 1985a; Diekmann & Wang, 1985; Diekmann, 1986; for a review, see Hagerman (1990a)]. The electrophoretic approach is based on the observation that DNA molecules are retarded on polyacrylamide gels (lower electrophoretic mobility) to an extent that depends on the degree of axial curvature of those molecules. This approach has been extended to the study of tertiary (branched) structures in DNA (Cooper & Hagerman, 1987, 1989; Duckett et al., 1988), and more recently to the determination of the helix repeat of dsRNA in solution (Tang & Draper, 1990; Bhattacharyya et al., 1990). The helix repeat so determined, ca. 11.5–12.0 bp/turn, is in accord with values estimated from the fiber diffraction patterns of RNA (Arnott et al., 1968, 1973).

Although the electrophoretic approach is a sensitive means for detecting axial curvature, and has been used for the quantitative analysis of helix repeat/phasing in both DNA and RNA, it has as its principal shortcoming the inability to provide accurate estimates for the magnitude of curvature (Hagerman, 1990a). In contrast, the second experimental approach, transient electric birefringence (TEB), largely circumvents the problems of quantitation associated with the gel approach. In brief, TEB measures the rates of rotational diffusion of molecules of interest following the removal of a brief, orienting electric field pulse (Fredericq & Houssier, 1973; Hagerman, 1985b). This approach has been shown to be a sensitive, quantitative means for determining the helix parameters of DNA in solution (Elias & Eden, 1981; Hagerman, 1981; Hagerman & Zimm, 1981), and has been used to characterize both altered helix elements (Hagerman, 1984; Levene et al., 1986) and tertiary structure (Cooper & Hagerman, 1989) in DNA.

In the current work, the T7 transcription system has been used in conjunction with both gel electrophoretic and hydrodynamic (TEB) approaches to examine the properties of several dsRNA molecules. In the first phase of this study, the construction of the transcription vectors has capitalized on the observation that the preferred T7 transcription start sequence, 5′-GGGAG, can be made complementary to the transcript terminus if the transcription stop is created by *Sma*I cleavage (CCC/GGG) and an *Eco*RV restriction site (GAT/ATC) is used as the cloning site. Thus, transcripts would all have the form, GGGAGAU-insert-AUCUCCC. Transcripts obtained from vectors into which the insert DNA has been cloned in both orientations would therefore yield, when annealed and purified, fully duplex double-stranded (ds) RNA molecules. The choice of the transcription start and termination sequences was guided by the work of Draper et al. (1988), who demonstrated that the *Sma*I (DNA) 3′ terminus yielded the greatest fraction of correct (full-length) 3′ RNA termini.

The production of dsRNA molecules directly from the primary transcripts eliminates the need for nuclease (e.g., endonuclease T_1; Tang & Draper, 1990) trimming of the 5′ ends of annealed transcripts prior to electrophoretic or hydrodynamic analysis. While nuclease trimming would not be expected to present difficulties for the fully duplex molecules employed in the current study, such treatment may present difficulties when applied to dsRNA molecules possessing, by design, internal loops, branches, or other single-stranded regions.

In the second phase of the current study, the electrophoretic and hydrodynamic properties of several dsRNA molecules are examined. For one such molecule, containing a series of four A_5·U_5-tracts spaced at 12 bp intervals (12 bp being close to the observed helix repeat of 11.5–12.0 bp/turn; Tang & Draper, 1990; Bhattacharyya et al., 1990), there is no indication by either electrophoretic or hydrodynamic behavior that such A-tracts generate curvature in the helix axis of dsRNA, in contrast to the effects of such A-tracts in DNA.

Materials and Methods

Synthesis and Isolation of DNA. Chemicals, unless otherwise specified, were of analytical grade and were purchased from Sigma or Fisher Scientific. Enzymes were purchased from Bethesda Research Laboratories, New England Biolabs, or Promega Biotech. DNA oligonucleotides were synthesized and detritylated on a Milligen/Biosearch 8750 DNA synthesizer, followed by cleavage from the CPG support and deprotection with concentrated ammonium hydroxide. The deprotected oligonucleotides were purified on 2-mm-thick, 25-cm-long 8 M urea gels (14–20% polyacrylamide). DNA bands were visualized by UV shadowing onto a fluorescent thin-layer chromatography plate. The bands were excised and macerated, and the DNA was eluted by soaking overnight in H_2O. The DNA was further purified and concentrated on DE 52 columns (Whatman) using 0.2 M triethylammonium acetate, pH 7 (TEAA), for the wash and 2 M TEAA for elution. The buffer was evaporated in a Speedvac (Savant), and the oligonucleotides were washed with 50% ethanol and dried.

Complementary DNA oligonucleotides were annealed by mixing approximately 0.1 mg/mL each strand in TE buffer (10 mM Tris-HCl, pH 8, and 1 mM EDTA), heating the mixture to 90 °C for 10 min, and cooling to room temperature over a period of at least 30 min. Phosphorylation (T4 polynucleotide kinase; 1 h, 37 °C) and ligation (T4 DNA ligase, overnight, 25 °C) reactions were carried out in 50 mM Tris-HCl, pH 7.8, 10 mM $MgCl_2$, 5 mM DTT, and 1 mM ATP, followed by extraction with phenol/chloroform and precipitation (0.3 M sodium acetate and 1 volume of 2-propanol). Purification of duplex DNA fragments was effected by excising DNA-containing bands from nondenaturing polyacrylamide gels (running buffer, 0.5× TBE: 45 mM Tris–borate, pH 8.3, and 1.25 mM EDTA), followed by electroelution (1–2 h, 0.5× TBE, 250 V) onto a 1-mL DE 52 column and subsequent elution with TEAA as described above.

Cloning, Plasmid Purification, and Characterization of Plasmid Constructs. Plasmid pBR328 (Balbas et al., 1986) was cleaved with *Eco*RI/*Hin*dIII, or with *Eco*RI/*Eco*RV, and the large fragments purified on agarose gels in the following manner: The appropriate bands were excised from the gel, vigorously shaken with an equal amount of phenol, and frozen. The agarose was then spun down, leaving a solution containing the plasmid fragment (ca. 60% yield) which was subsequently extracted with chloroform and precipitated with 2-propanol.

DNA oligonucleotides, if present following the construction of DNA inserts, were removed by passage of ligation reactions over conventional 0.5 × 18 cm Sephadex G-50 columns before ligation of the inserts to the purified plasmid fragments. Ligated plasmids were used to transform *E. coli* HB101 (grown on LB agar containing 50 μg/mL ampicillin). Mi-

[1] Abbreviations: ATP, adenosine 5′-triphosphate; *b*, hydrodynamic radius; bp, base pair(s); BSA, bovine serum albumin; ds, double stranded; DTT, dithiothreitol; EDTA, ethylenediaminetetraacetate; EtdBr, ethidium bromide; *h*, helix rise (angstroms per base pair); kV, kilovolts; ln, natural logarithm; MOPS, 3-(*N*-morpholino)propanesulfonic acid; nt, nucleotide(s); PAGE, polyacrylamide gel electrophoresis; *P*, persistence length; P_i, inorganic phosphate; rNTP, ribonucleotide 5′-triphosphate; SD, standard deviation(s); τ, decay time; TEB, transient electric birefringence.

nipreps were characterized by restriction mapping.

Plasmids were isolated from 1–3 L of chloramphenicol-amplified LB/ampicillin cultures by using the alkaline lysis method (Birnboim & Doly, 1979) with subsequent treatment with RNase A, precipitation of the plasmid DNA with poly(ethylene glycol) (Hillen et al., 1981), phenol extraction, and ethanol precipitation. The DNA, 0.5–2 mg/L of culture, was about 60% superhelical with no detectable RNA and less than 10% contaminating chromosomal DNA.

Double-strand sequencing was performed by using the dideoxy procedure of Sanger et al. [1977; modified by Chen and Seeburg (1985)] using 3–4 μg of denatured plasmid, 2–3 ng of primer, 0.1 unit/μL Klenow fragment (20 min), and the New England Biolabs' ^{35}S dideoxy sequencing mix. Sequencing was performed on both strands in order to eliminate possible sequence errors.

In Vitro Transcription and Analysis of dsRNAs. For in vitro transcription reactions, the template-containing plasmids were cleaved overnight at 30 °C with 0.2 unit/μL *Sma*I (BRL) in 20 mM Tris-HCl, pH 7.4, 5 mM $MgCl_2$, 50 mM KCl, and 0.1 mg/mL BSA. The linearized plasmids were then phenol/chloroform-extracted, followed by precipitation with 1 volume of 2-propanol and 0.1 volume of sodium acetate. T7 RNA polymerase, kindly provided by Dr. Olke Uhlenbeck, was approximately 50% pure, and demonstrated very low RNase and DNase activity (polymerase concentrations refer to total protein). Transcription reactions were performed by using the protocol of Milligan et al. (1987) with slight modifications. The reaction mix consisted of 40 mM Tris-HCl, pH 7.8, 25 mM $MgCl_2$, 2 mM spermidine, 5 mM DTT, 0.01% Triton X-100, 0.05 mg/mL BSA, 3–4 mM (final) of each rNTP, 0.05–0.1 mg/mL cleaved plasmid, and 0.05–0.1 mg/mL T7 RNA polymerase. After 1–3-h incubation at 37 °C, the reactions were stopped by the addition of EDTA to a final concentration of 50 mM, followed by phenol/chloroform extraction and 2-propanol precipitation. Neither prior treatment of the plasmid with RNase nor contamination with chromosomal DNA interfered with the transcription reactions. The RNA transcripts were separated from nucleotides, oligomers, and DNA (with regeneration of the plasmid) on a Qiagen column (Qiagen-pack 100, Diagen, Dusseldorf, FRG) according to the manufacturer's instructions.

Transcripts (approximately 0.3 mg/mL of transcription mix, corresponding to more than 100 rounds of transcription per template plasmid) were typically 80–90% pure as judged by denaturing gel electrophoresis. Furthermore, purification of the single strands on denaturing gels prior to annealing had no significant effect on the quality of the final duplex product. Therefore, annealing reactions were generally performed without further purification. Melting experiments (Gast and Hagerman, unpublished observations) had revealed that some salt is needed for proper hybridization and that melting points of the constructs were close to 90 °C. Thus, annealing was carried out by incubating equal amounts (ca. 0.5–0.7 mg/mL) of each RNA transcript in 10 mM Tris-HCl, pH 6.5, 100 mM NaCl, and 1 mM EDTA for 10 min at 95 °C, followed by slow cooling (>30 min) to room temperature. The annealing product consisted of one major band and a light smear at higher molecular weights, presumably alternative conformers and single strands.

Double-stranded RNAs were purified to greater than 95% homogeneity on 6–8% native polyacrylamide gels in 0.5× TBE buffer and were excised (following brief UV-shadowing) and electroeluted as described above, except that elutions were carried out in 1× TBE, adjusted to pH 7.6 with boric acid. The DE 52 columns were washed with 0.2 M TEAA and the dsRNAs eluted with 1 M NaCl in 0.2 M TEAA and precipitated with 1 volume of 2-propanol. Desalting was accomplished by spinning 0.2 mL of the RNA solution through a 1.2 × 2.5 cm G-25 (medium) column (Pharmacia) in a table-top centrifuge for 2 min at 1000 rpm, with subsequent washing (3 times) with 0.2 mL of H_2O as described above. The collected eluant was then concentrated to the original volume by partial evaporation in a Speedvac (Savant). Yields were typically 20–50 μg of double-stranded RNA from 2 × 0.5 mL transcriptions. Purified and desalted dsRNA was stable for months at 4 °C.

Once formed, quantities of dsRNA molecules sufficient for EtdBr staining were not readily melted on denaturing (8 M urea, 60 °C) gels. Therefore, in order to estimate the amount of full-length transcript, either Qiagen-purified transcription products or purified dsRNAs (after TEB experiments) were treated with alkaline phosphatase, and 5′-end-labeled with [γ-^{32}P]ATP (DuPont-NEN) according to standard procedures (Maniatis et al., 1982). The unincorporated ATP was removed either on Qiagen columns or on Sephadex G-25 spin columns (Maniatis et al., 1982). Electrophoresis of the 5′-end-labeled transcription products on denaturing polyacrylamide gels revealed a major band corresponding to full-length transcript, and a ladder of additional failure bands, whereas purified double strands ran as a single band corresponding to the full-length transcript (in the case of the 180 bp dsRNA, a few faint failure bands remained, <5%).

S_1 nuclease digestions were performed for 5–60 min in 50 mM sodium acetate, pH 4.5, 3 mM $ZnCl_2$, 300 mM NaCl, ca. 0.2 unit/mL S_1, and 0.1–0.2 mg/mL unlabeled tRNA. The products were identified on sequencing gels.

Gel Electrophoresis. Analytical nondenaturing gel electrophoresis was performed on 1-mm slab gels, using either 0.5× TBE (≈10 V/cm) at room temperature (24 ± 1 °C) or TEB buffer (5 mM NaP_i, pH 7.2, and 0.125 mM EDTA) with buffer recirculation at 8 ± 1 °C in the coldroom. An acrylamide:bis(acrylamide) ratio of 29:1 (0.1% TEMED and 0.07% ammonium persulfate) was used throughout the current study. The gels were stained with ethidium bromide and photographed on a UV transilluminator.

Relative mobilities, μ_{rel}, were determined as the ratio of the distance traveled by a certain dsRNA molecule and the distance traveled by electrophoretically normal DNA molecules having the same number of base pairs. This latter distance was determined from a calibration curve in which the ln bp of DNA standards (in the range of 0.05–0.6 kbp) was plotted versus the migration distance. The linear regression of this curve resulted in correlation coefficients of better than −0.995. DNA standards generated from pBR328 showed no anomalous electrophoretic behavior nor did the DNA constructs for pFUB or pFU3A.

Transient Electric Birefringence Measurements. Birefringence measurements were carried out by using an instrument substantially identical with the one described by Hagerman (1985b). Concentrations of dsRNA were generally in the range of 40–80 μg/mL (6–12 μg in the 160-μL birefringence cell). All experiments were performed at 4.0 ± 0.2 °C using buffer conditions as described in the text and figure/table legends. Rectangular electric pulses ranged from 0.5 to 1.75 kV (field strength, E = 2.5–8.75 kV/cm for the 2-mm electrode gap), and were 2.5–3.0 μs in duration. Intervals between pulses were generally at least 10–15 s in order to avoid joule heating of the samples. The birefringence decay curves were accumulated and averaged on a Tektronix 7603 oscilloscope,

Table I: DNA Sequences Used in the Current Study[a]

Designation	Sequence
Adapter A_L	aattT AATAC GACTC ACTAT AGGGA G
Adapter A_R	CTCCC GGGT
35 bp insert	aattA ATACG ACTCA CTATA GGGAG ATATC TCCCG GG
212 bp insert	CCGTC TTCAT TTCCA TGCGG TGCAC TTTAT GCGGA CACTT CCTAC AGGTA GCGTT GACCC TAATT TTGGT CGTCG GGTAC GCAAT CGCCG CCAGT TAAAT AGGGA ATTCC CCGTC TTCAT TTCCA TGCGG TGCAC TTTAT GCGGA CACTT CCTAC AGGTA GCGTT GACCC TAATT TTGGT CGTCG GGTAC GCAAT CGCCG CCAGT TAAAT AG
122 bp insert	ATCGG CCTCG GCTGT GCCTG CCTTA GATTC ATATG ACTAC TTGGA GGAGC TCTAG CATAA GCTTA CGGTA ATCAT CACAA GTGAG ATACC TCGCG ATTCA GCTGA CGCTA CTGCT GGCCG AT
44 bp insert	agctA AAAAT GGAGG TAAAA AGTTC GATAA AAAGA ATTCG AAAA

[a] Unless otherwise noted, all sequences represent only one strand of a double-stranded molecule. Sequences are written 5′ to 3′. Lower case letters indicate unpaired bases. Boldfaced sequences indicate the T7 promoter and conserved transcription start sequence in the A_L adapter and 35 bp insert. Underlined sequences indicate restriction sites and site-compatible ends, in order from left to right. A_L, pseudo-*Eco*RI end; A_R, *Sma*I (the complementary strand of A_R possess the *Hin*dIII-compatible, single-strand overhang, 5′-agct); 35 bp insert, pseudo-*Eco*RI end, *Eco*RV, *Sma*I; 212 bp insert, *Eco*RI; 122 bp insert, *Eco*RV end, *Nde*I, *Sac*I, *Hin*dIII, *Pvu*II, *Eco*RV end; 44 bp insert, pseudo-*Hin*dIII end, *Eco*RI (the complementary strand possesses the single-strand, *Hin*dIII-compatible overhang, 5′-agct). The sequence between the A-tracts corresponds to the variable-loop/D-stem-loop region of $tRNA^{Phe}$ (yeast) (Sampson et al., 1989). The fifth A residue of the fourth A-tract is provided by the *Hin*dIII site, A/AGCTT.

transferred to an IBM PC/AT microcomputer, and processed by using a modified version of the scientific software, ASYST (Macmillan Software Co., New York, NY). Base lines were corrected for all measurements by subtracting the buffer response curve from the sample curve. The decay times, τ, were determined from the linear (terminal) portion of a ln $[n(t)/n(0)]$ vs t plot, where t is the elapsed time following removal of the field, $n(t)$ is the birefringence signal at time t, and $n(0)$ is the signal strength at the time the field is turned off (see the legend to Figure 3). Since τ values were observed to be independent of field strength for the range used in this study, the mean ± 1 SD values of τ were determined from a series of values representing both repeat measurements at the same field strength and measurements performed at different field strengths. The dsRNAs used in the birefringence experiments were analyzed on both nondenaturing and denaturing polyacrylamide gels. No signs of degradation could be detected even after more than 100 field pulses (Figure 1).

Results

Construction of T7 Promoter Transcription Vectors for the Production of dsRNA Molecules. Transcription vectors possessing a T7 promoter and optimal start sequence, 5′-GGGAG (Milligan et al., 1987; Draper et al., 1988), and a downstream (transcription-terminating) *Sma*I restriction site, were constructed by using two closely related approaches. In the first approach, two adapters (Table I) were used to insert a 212 bp fragment between the *Eco*RI and *Bam*HI sites of pBR328 (Balbas et al., 1986). One adapter (A_L) contains both the T7 promoter and the GGGAG start sequence; the second adapter (A_R) contains the *Sma*I site. The insert itself (Table I) comprises two, 102 bp direct repeats (the 102 bp sequence was originally derived from ϕX174; Shore et al., 1981) divided by a central 8 bp *Eco*RI linker, the latter providing a point for the insertion of additional sequences. The resulting vectors (possessing the 212 bp insert in both orientations) are designated pFUH0A and pFUH0B (Table II), and each yields 222-nt transcripts that are complementary to one another.

Table II: Compilation of the Plasmid Constructs

plasmid designation	insert (bp)[a]	host plasmid/site[b]	transcript (nt)
pFU1	35	pBR328/*Eco*RI–*Eco*RV	14
pFUH0A, pFUH0B[c]	A_L-212-A_R	pBR328/*Eco*RI–*Hin*dIII	222
pFUA, pFUB	212	pFU1/*Eco*RV	226
pFU3A, pFU3B	122	pFU1/*Eco*RV	136
pFU3A-7, pFU3B-8	44	(pFU3A, pFU3B)/*Eco*RV	180

[a] Inserts and adapters are delinated in Table I. [b] For those instances where two enzyme recognition sites are indicated, the intervening fragment from the host plasmid has been deleted. [c] The pairs of plasmids are related by opposite orientation of the insert.

The second approach consists of two parts: namely, (i) the construction of a general cloning/transcription vector, pFU1, by insertion of a 35 bp synthetic fragment (35 bp insert; Table I) between the *Eco*RI and *Eco*RV sites of pBR328; and (ii) the subsequent insertion of blunt-ended fragments (212 or 122 bp; Table I) into the newly created *Eco*RV site of pFU1, the original *Eco*RV site of pBR328 having been destroyed during the formation of pFU1. The resulting vectors are listed in Table II. It should be noted that due to the presence of the *Eco*RV site in pFU1, transcripts derived from vectors pFUA and pFUB are four nucleotides longer than those produced from pFUH0A and pFUH0B, although both templates contain the 212 bp insert.

Finally, an additional 44 bp fragment possessing four tracts of $(dA)_5$·$(dT)_5$ spaced at 12 bp intervals (Table I) was inserted into the central *Hin*dIII site of pFU3A and pFU3B to yield pFU3A-7 and pFU3B-8, respectively (Table II). The rationale for using the 122 bp containing template (pFU3 derivatives) was that the transcripts derived from that template would not have runs of greater than two contiguous A (or U) residues, other than those produced from inserts at the *Hin*dIII site, and so would not have the potential to mask any electrophoretic or hydrodynamic effects of the central A-tracts in the dsRNA molecule. It is uncommon to find naturally occurring templates that do not contain runs of more than two contiguous A residues (see, for example, the sequence of the 212 bp fragment; Table II). The 122 bp sequence itself (excluding the *Eco*RV sites) was therefore generated as random sequence, subject to the constraints that the *Hin*dIII site would be preserved and that no runs of greater than two contiguous A or G residues would be permitted.

Production and Characterization of dsRNAs Used in This Investigation. In order to reduce the losses incurred through gel purification of the single-stranded RNA transcripts, the transcripts were not routinely purified prior to annealing. In most transcription reactions, at least 80–90% of the RNA was the desired product, with some of the remaining RNA comprising very long (several kilobases) transcripts, presumably read-through transcripts from residual uncleaved plasmid, and very short (10–20 nt) transcripts produced by abortive initiation. The bulk of these contaminating RNAs, as well as the plasmid DNA, was removed by passing the nucleic acid mixture over Quiagen columns. This partially purified ma-

Table III: Relative Mobilities, μ_{rel}, of the dsRNA Molecules Compared to DNA Standards[a]

buffer[b]	gel (%)[c]	dsRNA length (bp) 136	180	222	"224"	226
	4	0.90	0.90	0.89		0.89
	6	0.89	0.90	0.90	0.89	0.90
	8	0.87	0.88	0.89	0.90	0.90
	10	0.84	0.87	0.87		0.89
	12	0.83	0.85	0.87	0.84	0.86
	16	0.76	0.77			0.70
0.8 V/cm	6	0.89	0.89			0.92
8 °C	12	0.75	0.76			0.79
31 °C	12	0.85	0.88	0.90	0.88	0.91
50 mM NaCl	8	0.84	0.85	0.89		0.90
100 mM NaCl	8	0.79	0.80	0.84		0.85
250 mM NaCl, 8 °C	8	0.70	0.70	0.70		0.71
5 mM $MgCl_2$	4	0.88	0.88	0.88		0.87
5 mM $MgCl_2$	6	0.85	0.85	0.86	0.84	0.86
5 mM $MgCl_2$	8	0.82	0.82	0.84		0.85
5 mM $MgCl_2$	12	0.73	0.77			0.78
	0.6% agarose	0.93	0.93			0.93

[a] μ_{rel} is defined in the text. The majority of the numbers were determined from at least two electrophoresis runs. [b] Conditions specified in the "buffer" column represent alterations from the standard buffer/running conditions: 0.5 × TBE, 24 ± 1 °C, 10 V/cm. [c] Acrylamide gel concentration unless specified otherwise.

Table IV: Values for Relative Mobility, μ_{rel}, Determined under Buffer Conditions Identical with Those Used for the Electric Birefringence Experiments[a]

buffer[b]	gel (%)[c]	dsRNA length (bp) 136	180	222	"224"	226
	8	0.80	0.81	0.83	0.83	0.86
	12	0.72	0.75	0.70	0.70	0.77
25 °C	8	0.86	0.87	0.90	0.90	0.91
1 mM $MgCl_2$	8	0.75	0.75	0.79	0.77	0.80
1 mM $MgCl_2$, 0.5 mM spermidine	8	0.76	0.78	0.82		0.82
0.5 × TE	8	0.81	0.83	0.88		0.87

[a] Standard buffer conditions: 5 mM NaP_i, pH 7.2, and 0.125 mM NaEDTA; field strength, 10 V/cm; temperature, 8 ± 1 °C. [b] Changes from standard buffer conditions are listed, except for 0.5 × TE (5 mM Tris-HCl, pH 8.0, and 0.5 mM NaEDTA), which represents a buffer substitution. [c] Polyacrylamide gel.

terial was then annealed and gel-purified to yield dsRNAs that were greater than 95% pure.

The purity of the dsRNA species was established by several means: (1) The RNA strands comprising the double-stranded molecule are the correct length on denaturing gels when compared to denatured DNA standards (data not shown). (2) The purified band is the only one observed on UV-shadowing gels, demonstrates S_1 resistance, and exhibits greater fluorescence with ethidium than an equal quantity of either of the single-stranded transcripts. (3) Each pair of transcripts anneals in a stoichiometric manner as judged by ratio-mixing experiments on nondenaturing gels (data not shown). (4) Melting experiments using the purified dsRNA molecules demonstrate a single, sharp transition at higher temperatures (T_m >90 °C at 100 mM NaCl) than DNA molecules of comparable length (Gast and Hagerman, unpublished results). It should be noted that the melting transitions of the dsRNA molecules demonstrate a significant hysteresis upon cooling for salt concentrations below 100 mM. Annealing the transcripts under these same low-salt conditions results in a mixture of products which consists of one major band and a smear extending to higher molecular weights. The smear, which probably consists of incompletely annealed transcripts, is sensitive to nuclease S_1, whereas the major band is resistant to S_1. It should be noted that annealing reactions performed in the presence of 100 mM NaCl and/or 5 mM $MgCl_2$ result in drastically reduced amounts of S_1-sensitive material.

Reduced Electrophoretic Mobilities of dsRNA Molecules on Polyacrylamide Gels. A characteristic of all of the dsRNAs examined in the current study is a lower electrophoretic mobility on nondenaturing polyacrylamide gels relative to DNA fragments having the same number of base pairs (Tables III and IV, Figure 1). This general phenomenon for dsRNA has been reported previously (Biebricher et al., 1982; Bhattacharrya et al., 1990). By contrast, the single strands nearly comigrate with their DNA counterparts on denaturing gels (not shown).

It should be noted that in the current study the electrophoretic behavior of dsRNA molecules is reported as the mobility ratio, μ_{rel}, a dimensionless quantity defined as the ratio of the distances traveled by dsRNA and DNA molecules having the same number of base pairs ($\mu_{rel} = \mu_{dsRNA}/\mu_{DNA}$). This quantity represents a more direct reflection of the physical processes taking place in the gel than previous quantities, used by ourselves and others to describe the mobilities of A-tract DNA, which expressed retardation in terms of the apparent number of base pairs.

Several potential sources of the reduced mobilities (μ_{rel} < 1.0) of the dsRNA molecules were examined; the results are displayed in Table III and Figure 2. It is clear from the polyacrylamide gel concentration dependence that there is a very gradual reduction in μ_{rel} with increasing gel concentration, with the reductions in the presence of Mg^{2+} being slightly greater than in its absence. Preincubation of the dsRNA molecules with Mg^{2+} and/or spermidine does not alter the mobility of those molecules on non-Mg^{2+} gels (Figure 1), suggesting that the bulk of the associated counterions is readily exchanged during the course of the electrophoresis experiment. In contrast to the modest dependence of μ_{rel} on gel concentration observed with dsRNA molecules, single-stranded RNA molecules exhibit a range of μ_{rel} values with different gel concentrations, presumably reflecting varying degrees of

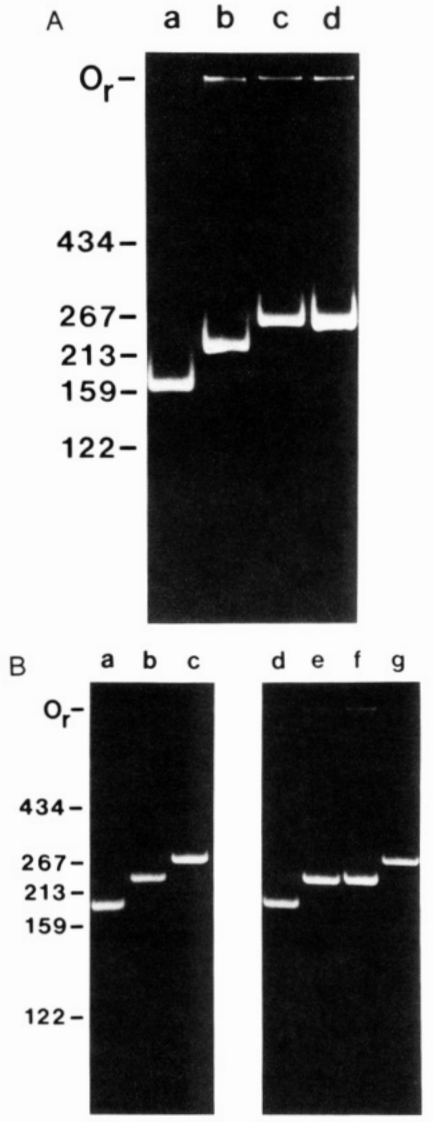

FIGURE 1: Sample electrophoretic patterns (on 8% polyacrylamide gels) of several dsRNA molecules employed in the current study. (Panel A) 0.5× TBE buffer at room temperature: (lane a) 136 bp dsRNA (after TEB experiments); (b) 180 bp (A-tract) dsRNA; (c) 226 bp dsRNA (after TEB experiments); (d) "224 bp" mismatched dsRNA. (Panel B) TEB (birefringence) buffer at 8 °C: (lane a) 136 bp dsRNA; (b) 180 bp dsRNA; (c) 226 bp dsRNA; (d) 136 bp dsRNA after TEB in the presence of magnesium and magnesium + spermidine; (e) 180 bp dsRNA after TEB with magnesium alone; (f) 180 bp dsRNA after TEB in the presence of magnesium and spermidine; (g) 226 bp dsRNA after TEB in 1–4 mM magnesium. Representative DNA band sizes (bp) are indicated to the left; O_r, gel origin.

secondary structure formation (results not shown). Extrapolation of μ_{rel} to 0% acrylamide gel concentration yields a value of 0.92 ± 0.01 (Figure 2). This value probably reflects the lower net charge per phosphate of dsRNA relative to DNA; however, several factors undoubtedly contribute to this extrapolated value (see Discussion).

Finally, hybridization of the transcripts from pFUH0A and pFUB, or from pFUH0B and pFUA (Table II), results in two base bulges near both ends of the annealed molecule:

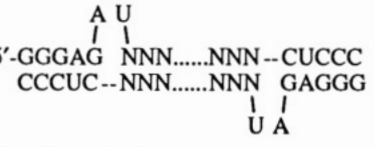

The electrophoretic behavior of this heteroduplex molecule

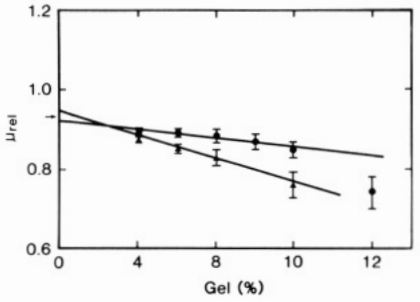

FIGURE 2: Plots of the relative electrophoretic mobilities, μ_{rel} (averaged for all dsRNAs listed in Table III), as a function of acrylamide gel concentration. (●) Absence of magnesium; (▲) presence of 5 mM $MgCl_2$; (→) 0.6% agarose gel in the absence of magnesium. Error bars represent ±1 SD from the mean value. For the extrapolation to 0% gel, a linear least-squares fit was performed by using data points for 4–10% acrylamide gels.

Table V: Transient Electric Birefringence Decay Times, $\tau_{20,w}$, (μs), of dsRNA Molecules[a]

buffer[b]	dsRNA length (bp)		
	136	180	226
	1.21 ± 0.09	2.12 ± 0.09	3.55 ± 0.14
10 mM NaCl		2.17 ± 0.15	3.40 ± 0.13
25 mM NaCl	1.16 ± 0.07		
1 mM $MgCl_2$[c]	1.08 ± 0.05	1.90 ± 0.06	3.46 ± 0.08
2 mM $MgCl_2$			3.45 ± 0.11
4 mM $MgCl_2$			3.43 ± 0.13
1 mM $MgCl_2$, 0.5 mM spermidine	1.06 ± 0.07	1.98 ± 0.11	3.35 ± 0.23

[a] Decay times were determined under buffer conditions specified in Table IV, except for the temperature, which was 4.0 ± 0.2 °C for the birefringence measurements. Decay times (±1 SD) represent the terminal, log-linear portion of the decay curve (always in excess of 70% of the total decay curve). Actual decay times were converted to $\tau_{20,w}$ by the formula: $\tau_{20,w} = (\eta_{20,w}/\eta_T)(T/293)\tau_{obsd}$. [b] Buffer additions are as indicated. [c] $MgCl_2$ solutions were prepared by weighing fresh $MgCl_2 \cdot 6H_2O$.

("224 bp"; Figure 1A, Table III) is indistinguishable from its fully duplex counterparts, a result that is consistent with the relatively modest effects observed for dsRNA molecules possessing two, two-base bulges (out of phase) near the center of molecules (Tang & Draper, 1990). The absence of enhanced sensitivity to nuclease S_1 of the two-base bulges in the 224 bp molecule suggests that the duplex region encompassing the bulges is relatively intact, in agreement with results obtained with DNA (Bhattacharyya & Lilley, 1989).

Behavior of an A-Tract dsRNA Molecule on Polyacrylamide Gels. In an effort to examine the effects of phased A-tracts on the structure of dsRNA, the electrophoretic behavior of a molecule containing four $A_5 \cdot U_5$ tracts at 12 bp intervals (180 bp; Tables I and II) was examined as a function of gel concentration, counterion type, and temperature (Figure 1; Tables III and IV). There is clearly no electrophoretic abnormality associated with the presence of the A-tracts in the dsRNA molecule under any of the conditions tested; that is, the modest reductions in mobility observed for the 180 bp molecule are identical with the corresponding values observed for the other molecules in the set. Preliminary experiments also reveal that this molecule also has the same mobility as a related non-A-tract molecule of 177 bp (not shown).

Analysis of the Birefringence Decay Times of dsRNA Molecules. Transient electric birefringence measurements were performed on three dsRNA molecules, including the 180 bp A-tract-containing molecule, under several conditions of counterion concentration and type (compare with electrophoresis results performed in identical buffers; Table IV). The

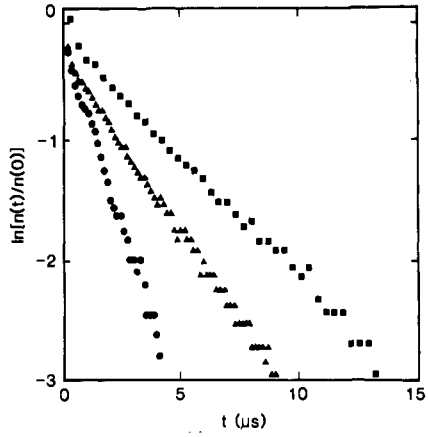

FIGURE 3: Representative data from transient electric birefringence experiments, with the decay of birefringence signal, $n(t)$, plotted as a function of time. Data are presented as semilogarithmic plots of the normalized birefringence signal, $n(t)/n(0)$, as a function of the elapsed time, t, following removal of the field; $t = 0$ actually corresponds to a time ca. 1.5 μs after the field was turned off (Cooper & Hagerman, 1989). (●) 136 bp dsRNA; (▲) 180 bp A-tract dsRNA; (■) 226 bp dsRNA. Buffer composition: TEB buffer (Table IV), 1 mM $MgCl_2$, and 0.5 mM spermidine; temperature, 4.0 ± 0.1 °C. Electric field pulse, 3.0 μs at 8.75 kV/cm.

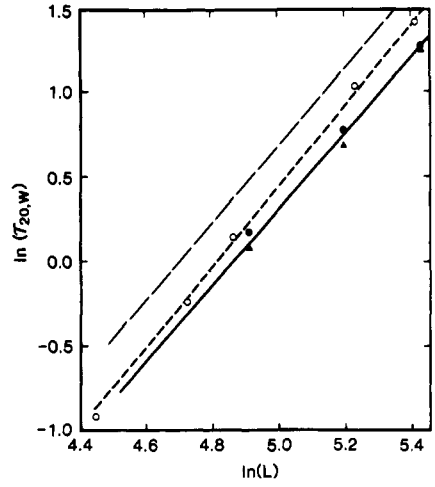

FIGURE 4: log–log plots of the dependence of $\tau_{20,w}$ on the number of base pairs, L, of the dsRNA molecules. Filled symbols represent pooled data from Table V, where (●) is no magnesium and (▲) is added $MgCl_2$ ± spermidine. The 1 SD values are given in Table V for the current data and average 5% (approximately twice the diameter of the filled circles) with a range of 3–7%. Open symbols (○) represent data from Biebricher et al. (1982), obtained in 1 mM sodium cacodylate, 1 mM NaCl, and 0.2 mM EDTA (20 °C). The dashed line represents a helix having $h = 3.4$ Å/bp and $P = 500$ Å, and corresponds to DNA. The short dashed line represents a best fit to the data of Biebricher et al. with $h = 2.8$ Å/bp and $P = 1800$ Å. The solid line represents a fit to the current data (combined, ±$MgCl_2$) with $h = 2.8$ Å/bp and $P = 600$ Å. As described in the text, the curves were generated by using eq 20–22 of Hagerman and Zimm (1981). The hydrodynamic radius was assumed to be 13 Å (see Discussion).

results of these TEB measurements are presented as terminal (longest) decay times, τ, in Table V. It should be noted that in all of the measurements performed in this study, the portion of the decay curve associated with τ was always equal to or greater than 70% of the total decay amplitude (Figure 3). Moreover, on the basis of measurements performed as a function of field strength for each of the dsRNA molecules depicted in Figure 3, the experimental decay times are strictly independent of the field strength of the orienting pulse for all three molecules (data not shown), in agreement with earlier observations (Hagerman, 1981).

It is evident from the data presented in Table V that the 180 bp dsRNA molecule displays hydrodynamic behavior that is entirely consistent with that of the 136 and 226 bp molecules (Figure 4); that is, the set of four phased A-tracts appears not to possess any significant degree of curvature of the helix axis. This observation stands in stark contrast to the results of TEB and TED (transient electric dichroism) measurements performed on A-tract DNA (Hagerman, 1984, 1990a; Levene et al., 1986) and is consistent with the absence of abnormal electrophoretic behavior of the A-tract dsRNA molecule.

It is also evident from the data presented in Figure 4 that the helix rise, h (in angstroms per base pair), is substantially smaller than the 3.4 Å/bp value determined for DNA under similar solution conditions (Hagerman, 1981). An analysis of the combined (±magnesium) data from the current study yields a value of 2.8 ± 0.1 Å for h(dsRNA). Moreover, our analysis of the data of Biebricher et al. (1982) yields essentially the same value. The current analysis is based on eq 20–22 of Hagerman and Zimm (1981), which yield the ratio, R_c, of the decay time, $\tau(h,P)$, for a molecule of helix rise, h, and persistence length, P (in angstroms), and the corresponding decay time, $\tau(h,\infty)$, for a rigid molecule [$R_c = \tau(h,P)/\tau(h,\infty)$]. Equating $\tau(h,\infty)$ to $\tau_B(h)$, where τ_B is computed from Broersma's formula (Broersma, 1960; Hagerman & Zimm, 1981), one obtains computed values for $\tau(h,P)$ from the expression:

$$\tau(h,P) = R_c(h,P)\tau_B(h) \quad (1)$$

The above expression has been used previously (Hagerman, 1981) to obtain values for the persistence length of DNA that are within 10% of the corresponding values determined by nonhydrodynamic means [for a review, see, Hagerman (1989)].

For $h = 2.8$ Å, the best (least-squares) value for P, based on the combined data (±Mg^{2+}) in Table V, is 600 Å. However, for this limited dataset, P is subject to a rather large degree of uncertainty, with a range of possible values extending from ca. 500 to 700 Å. It is interesting to note that the two datasets (Table V; +Mg^{2+} or −Mg^{2+}) yield slightly different slopes of ln τ vs ln L in Figure 4, with the +Mg^{2+} data displaying the greater slope. This last observation suggests that the presence of Mg^{2+} may result in a slight foreshortening and stiffening of the dsRNA helix; however, the effect appears to be of marginal significance for the relatively short molecules employed in the current study. Efforts are currently underway to examine this latter effect, as well as to refine the estimates for P and h, using a series of shorter and longer dsRNA molecules.

Discussion

In this paper, we have described the design and use of sets of general transcription vectors that will enable the production of blunt-ended, double-stranded RNA molecules directly from the transcripts without the need for enzymatic trimming. The basic vector, pFU1, was designed to facilitate the production of a wide variety of RNA molecules with duplex ends, while the interior sequences may or may not be duplex. The derivative vector set, pFU3A and pFU3B, was designed to provide a constant 122 bp dsRNA background within which additional helical or nonhelical elements could be located centrally. For the latter constructs, the 122 bp of dsRNA represents the RNA analogue of the in vitro "reporter-arm" constructions described in conjunction with studies of curved DNA (Wu & Crothers, 1984; Diekmann, 1986; Hagerman, 1988, 1990b). For studies of specific RNA sequences, one need only insert the analogue DNA sequences into the central *Hin*dIII site of pFU3A and pFU3B, or into the *Eco*RI site of

pFUA and pFUB, prior to transcription of those plasmids.

In a specific application of the above vectors to the study of RNA structure, the pFU3A/pFU3B plasmid set has been used to clone a series of A-tract repeats in order to evaluate the effects of such A-tracts on dsRNA structure. Specifically, a 44 bp synthetic DNA fragment (Table I) containing four A_5·T_5 tracts spaced at 12 bp intervals was inserted in both orientations into the *Hin*dIII site of pFU3A and pFU3B. The dsRNAs produced through transcription of the resulting constructs were analyzed both by polyacrylamide gel electrophoresis and by transient electric birefringence; no evidence of significant curvature of the dsRNA helix axis was obtained by either approach. This observation contrasts sharply with the behavior of DNA molecules containing phased A-tracts, the latter being associated with substantial curvature (Hagerman, 1990a). It is evident that the failure to observe curvature in RNA is not due to the difference between the helix repeat of RNA (ca. 11.5–12.0 bp/turn; Arnott et al., 1968, 1973; Tang & Draper, 1990; Bhattacharyya et al., 1990) and the A-tract spacing of the dsRNA construct (12 bp per A-tract repeat), since the difference for RNA is less than the difference for substantially curved, A-tract DNA molecules with a 10 bp A-tract repeat. It is also unlikely that the failure to observe curvature in dsRNA is due to temperature or ion effects, since studies were performed at temperatures ranging to below 10 °C, and were performed both in the presence and in the absence of $MgCl_2$.

In light of the above, the most likely explanation for our failure to detect A-tract-induced curvature in dsRNA is that it does not occur to any appreciable extent. This conclusion is in agreement with recent gel electrophoretic and electron micrographic findings of J. Griffith and co-workers (J. Griffith, personal communication). Those workers failed to detect appreciable curvature of dsRNA molecules derived from transcripts of kinetoplast DNA sequences containing phased A-tracts, although the A-tract phasing of those RNA molecules was different than that of the A-tract molecule employed in the current study. It is not apparent why A-tract RNA molecules should lack curvature, in contrast to their A-tract DNA counterparts. It is possible that, due to the restricted range of alternative conformations in RNA, junctional distortions between A-tract and non-A-tract sequences are much less pronounced than those observed in DNA.

The dsRNAs examined all display reduced electrophoretic mobilities in polyacrylamide gels when compared to DNA molecules having the same number of base pairs ($\mu_{rel} < 1.0$). Our findings are in accord with those reported for both agarose (Edmonson & Gray 1984) and polyacrylamide gels (Biebricher et al., 1982; Bhattacharyya et al., 1990); however, the origins of the lower mobilities of dsRNA molecules are not known. The reduced μ_{rel} values are not likely to be due to sequence-specific effects, since the effect appears to hold for all sequences studied thus far (Biebricher et al., 1982; Edmonson & Gray, 1984; Bhattacharyya et al., 1990). It should also be noted that μ_{rel} would be even smaller if RNA and DNA molecules of equal *length* were compared (e.g., 100 bp dsRNA, 2.8 Å/bp, vs 82 bp DNA, 3.4 Å/bp).

There are two properties generally ascribed to dsRNA that could result in lowered electrophoretic mobility, namely, reduced net charge and increased stiffness relative to DNA. The property of a reduced (relative) net charge of dsRNA is a direct prediction of the counterion condensation theory (Manning, 1978; Record et al., 1976, 1978) in which the residual charge per phosphate is proportional to the axial spacing of phosphate charges along the helix. Since the axial charge spacing for a dsRNA molecule having a helix rise of 2.8 Å/bp is only 1.4 Å/phosphate, the residual charge on the dsRNA molecule is expected to be only ca. 82% of the residual charge of DNA (1.7 Å/phosphate axial charge spacing); hence, one might expect the value of μ_{rel}, extrapolated to zero gel concentration, to be only 0.82. However, an opposing factor, one which would tend to increase the rate of migration of dsRNA relative to DNA in free solution, is the shorter axial length of dsRNA. Using the treatment of Tirado and Garcia de la Torre (1979) for the translation of a rigid cylinder, one obtains an expression for the translational friction coefficient, $\mathcal{F}$, of the form:

$$\mathcal{F} = 3\pi\eta\mathcal{L}/[\ln(\mathcal{L}/2b) + \gamma]$$

where $\mathcal{L}$ is the length of the cylinder, η is the solution viscosity, b is the cylinder radius (13 Å; see below), and γ is a numerical factor approximately equal to 0.35 for the range of dsRNA lengths employed in the current study (Tirado & Garcia de la Torre, 1979). Using a value of 2.8 Å/bp, as above, for the rise of dsRNA, one obtains the ratio $\mathcal{F}_{dsRNA}/\mathcal{F}_{DNA} = 0.87$; that is, a dsRNA molecule is expected to experience only ca. 87% of the frictional drag of a DNA molecule of the same number of base pairs. By assuming that μ_{rel} represents the product of these two opposing factors, one arrives at the value $\mu_{rel} = 0.82/0.87 = 0.94$, in remarkable agreement with the observed value of 0.92 ± 0.02 (Figure 2). It must be stressed that due to the rather large uncertainties associated with both the degree of charge neutralization and the relative friction coefficients, the agreement between the theoretical and experimental values must be regarded as fortuitous. It is also not known if the extrapolation to 0% gel concentration leads to a value which is meaningful for free electrophoresis. However, the above analysis does attest to the plausibility of the proposal that a reduced net charge on dsRNA is the basis for its reduced electrophoretic mobility ($\mu_{rel} < 1$; extrapolated to zero gel concentration). The above result also underscores the need for an independent determination of the extent of counterion condensation on dsRNA.

The second property generally ascribed to dsRNA, namely, reduced flexibility, can potentially affect the relative mobility of dsRNA in two ways. First, in the limit of zero gel concentration, reduced flexibility of dsRNA compared to DNA would tend to increase the ratio, $\mathcal{F}_{dsRNA}/\mathcal{F}_{DNA}$, thus lowering the expected value for μ_{rel}. Second, as has been discussed previously (Edmonson & Gray, 1984), the reduced mobility of dsRNA compared to DNA for a given gel concentration might be due to a greater intrinsic stiffness of dsRNA (Kapahnke et al., 1986). The proposal of Edmonson and Gray (1984) would appear to be qualitatively consistent with the observed lowering of μ_{rel} with increasing gel concentration (Figure 2). It is reasonable to suppose that a stiffer helix would experience more difficulty working its way through the gel matrix; however, this latter idea has yet to be tested rigorously. Furthermore, there is no conclusive evidence that under normal gel electrophoresis conditions dsRNA is substantially less flexible than DNA. In particular, the current birefringence decay results (Table V; Figure 4) suggest that the persistence length of dsRNA is only marginally increased over that of DNA. Moreover, the value of 1125 Å obtained for dsRNA by Kapahnke et al. (1986) probably represents an overestimate of the true value of the persistence length under the conditions employed in their sedimentation experiments, since those authors employed the expression of Yamakawa and Fuji (1973), which will lead to an overestimate of $s_{20,w}$, and hence to an underestimate for the coefficient of friction for a given persistence length (Zimm, 1980). In other words, fitting com-

puted values of $s_{20,w}$ to the corresponding experimental values will lead to an overestimate for P. It is clear that more detailed studies of the flexibility of dsRNA, coupled with a more quantitative description of the dependence of mobility on chain flexibility, will be needed before the dependence of μ_{rel} on gel concentration will be fully understood.

The relationship between the current birefringence decay results and those of Biebricher et al. (1982) should be noted (Figure 4). Within the limits of our combined experimental error, both sets of data are consistent with a helix rise of 2.8 ± 0.1 Å/bp; however, the τ values of Biebricher et al. increase more rapidly with increasing helix length than do those of the current study. The most straightforward explanation of this latter observation is that the persistence length of the dsRNA molecules is larger under the buffer conditions used by Biebricher et al. (1 mM sodium cacodylate, 1 mM NaCl, and 0.2 mM NaEDTA) than it is under the buffer conditions employed in the current study (Table V) [see Hagerman (1981)]. It is difficult to obtain a precise estimate for the persistence length of the dsRNA molecules under the buffer conditions used by Biebricher et al.; however, application of eq 1 to their data suggests that P is in excess of 1500 Å.

The value of 2.8 ± 0.1 Å/bp for the average rise of dsRNA in solution is in reasonable accord with previous determinations (ca. 2.7–3.0 Å/bp) using electron microscopy (Lang et al., 1987) and X-ray diffraction of fibers [Arnott et al. 1968, 1973; for a review, see Saenger (1984)] or crystals (Dock-Bregeon et al., 1988, 1989). Moreover, tRNAs exhibit a broad range of values for the local helix rise [1.7–3.1 Å/bp (Holbrook et al., 1978; Westhof et al., 1985)]. With regard to the helix radius of dsRNA, we have assumed a value of 13 Å, based on the largely equivalent structural radii for dsRNA and DNA (Saenger, 1984) and the hydrodynamic radius of 13 Å determined previously for DNA (Hagerman, 1981). However, rotational diffusion constants are only very weakly (logarithmically) dependent on the radius: for dsRNA molecules in the range 130–220 bp, a 1-Å change in the radius results in only a 4% change in the decay time.

Acknowledgments

We thank J. B. Mills for her assistance in the production of the synthetic oligonucleotides and for some of the cloning, B. Lieberman for writing a "random sequence" generating algorithm, and M. Wittenberger and Dr. Y. Hodges-Garcia for sequencing two of the plasmid clones. We are also indebted to Dr. D. E. Draper for providing information prior to its publication and for useful discussions, Dr. O. C. Uhlenbeck and his lab for a gift of T7 RNA polymerase, Drs. N. C. Stellwagen, J. P. Cooper, and G. Bellomy for their critical reading of the manuscript, and Dr. S. Diekmann for useful discussions regarding TEB.

Registry No. Poly(A), 24937-83-5; RNA polymerase, 9014-24-8.

References

Arnott, S., Fuller, W., Hodgson, A., & Prutton, I. (1968) *Nature 220*, 561–564.

Arnott, S., Hukins, D. W. L., Dover, S. D., Fuller, W., & Hodgson, A. R. (1973) *J. Mol. Biol. 81*, 107–122.

Balbas, P., Soberon, X., Merino, E., Zurita, M., Lomeli, H., Valle, F., Flores, N., & Bolivar, F. (1986) *Gene 50*, 3–40.

Bhattacharyya, A., & Lilley, D. M. J. (1989) *Nucleic Acids Res. 17*, 6821–6840.

Bhattacharyya, A., Murchie, A. I. H., & Lilley, D. M. J. (1990) *Nature 343*, 484–487.

Biebricher, C. K., Diekmann, S., & Luce, R. (1982) *J. Mol. Biol. 154*, 629–648.

Birnboim, H. C., & Doly, J. (1979) *Nucleic Acids Res. 7*, 1513–1523.

Broersma, S. (1960) *J. Chem. Phys. 32*, 1625–1635.

Chen, E. Y., & Seeburg, P. H. (1985) *DNA 4*, 165–170.

Chou, S.-H., Flynn, P., & Reid, B. (1989) *Biochemistry 28*, 2422–2435.

Cooper, J. P., & Hagerman, P. J. (1987) *J. Mol. Biol. 198*, 711–719.

Cooper, J. P., & Hagerman, P. J. (1989) *Proc. Natl. Acad. Sci. U.S.A. 86*, 7336–7340.

Davanloo, P., Rosenberg, A. H., Dunn, J., & Studier, F. W., (1984) *Proc. Natl. Acad. Sci. U.S.A. 81*, 2035–2039.

Denman, R., Negre, D., Cunningham, P. R., Nurse, K., Colgan, J., Weitzman, C., & Ofengand, J. (1989) *Biochemistry 28*, 1012–1019.

Diekmann, S. (1986) *FEBS Lett. 195*, 53–56.

Diekmann, S., & Wang, J. C. (1985) *J. Mol. Biol. 186*, 1–11.

Dock-Bregeon, A. C., Podjarny, A., Moras, D., de Bear, J. S., Gough, G. R., Gilham, P. T., & Johnson, J. E. (1988) *Nature 335*, 375–378.

Dock-Bregeon, A. C., Chevrier, B., Podjarny, A., Johnson, J., de Bear, J. S., Gough, G. R., Gilham, P. T., & Moras, D. (1989) *J. Mol. Biol. 209*, 459–474.

Draper, D. E., White, S. A., & Kean, J. M. (1988) *Methods Enzymol. 164*, 221–237.

Duckett, D. R., Murchie, A. I. H., Diekmann, S., von Kitzing, E., Kemper, B., & Lilley, D. M. J. (1988) *Cell 5*, 79–89.

Edmonson, S. P., & Gray, D. M. (1984) *Biopolymers 23*, 2725–2742.

Ehresmann, C., Baudin, F., Mougel, M., Romby, P., Ebel, J.-P., & Ehresmann, B. (1987) *Nucleic Acids Res. 15*, 9109–9128.

Elias, J. G., & Eden, D. (1981) *Macromolecules 14*, 410–419.

Fredericq, E., & Houssier, C. (1973) *Electric Dichroism and Electric Birefringence*, Clarendon, Oxford, U.K.

Greider, C. W., & Blackburn, E. H. (1989) *Nature 337*, 331–337.

Guerrier-Takada, C., Gardiner, K., Marsh, T., Pace, N., & Altman, S. (1983) *Cell 35*, 849–857.

Guerrier-Takada, C., Lumelsky, N., & Altman, S. (1989) *Science 246*, 1578–1584.

Hagerman, P. J. (1981) *Biopolymers 20*, 1503–1535.

Hagerman, P. J. (1984) *Proc. Natl. Acad. Sci. U.S.A. 81*, 4632–4636.

Hagerman, P. J. (1985a) *Biochemistry 24*, 7033–7037.

Hagerman, P. J. (1985b) *Methods Enzymol. 117*, 198–219.

Hagerman, P. J. (1988) *Unusual DNA Structures* (Wells, R. D., & Harvey, S. C. Eds.) pp 224–236, Springer-Verlag, New York.

Hagerman, P. J. (1989) *Annu. Rev. Biophys. Chem. 17*, 265–286.

Hagerman, P. J. (1990a) *Annu. Rev. Biochem. 59*, 755–781.

Hagerman, P. J. (1990b) *Biochemistry 29*, 1980–1983.

Hagerman, P. J., & Zimm, B. H. (1981) *Biopolymers 20*, 1481–1502.

Heus, H. A., Uhlenbeck, O. C., & Pardi, A. (1990) *Nucleic Acids Res. 18*, 1103–1108.

Hillen, W., Klein, R. D., & Wells, R. D. (1981) *Biochemistry 20*, 3748–3756.

Holbrook, S. R., Sussman, J. L., Warrant, R. W., & Kim, S.-H. (1978) *J. Mol. Biol. 123*, 631–660.

Kapahnke, R., Rappold, W., Desselberger, U., & Riesner, D. (1986) *Nucleic Acids Res. 14*, 3215–3228.

Lang, D., Steely, H. T., Kao, C.-Y., & Ktistakis, N. T. (1987) *Biochim. Biophys. Acta 910*, 271–281.

Levene, S. D., Wu, H.-M., & Crothers, D. M. (1986) *Biochemistry 25*, 3988-3995.
Malim, M. H., Tiley, L. S., McCarn, D., Rusche, J. R., Hauber, J., & Cullen, B. R. (1990) *Cell 60*, 675-683.
Maniatis, T., Fritsch, E. F., & Sambrook, J. (1982) *Molecular Cloning, A Laboratory Manual*, Cold Spring Harbor Laboratory, Cold Spring Harbor, NY.
Manning, G. S. (1978) *Q. Rev. Biophys. 11*, 179-246.
Milligan, J. F., Groebe, D. R., Witherell, G. W., & Uhlenbeck, O. C. (1987) *Nucleic Acids Res. 15*, 8783-8798.
Moazed, D., Stern, S., & Noller, H. F. (1986) *J. Mol. Biol. 187*, 399-416.
Murphy, F. L., & Cech, T. R. (1989) *Proc. Natl. Acad. Sci. U.S.A. 86*, 9218-9222.
Puglisi, J. D., Wyatt, J. R., & Tinoco, I. (1990) *Biochemistry 29*, 4215-4226.
Record, M. T., Jr., Lohman, T. M., & de Haseth, P. (1976) *J. Mol. Biol. 107*, 145-158.
Record, M. T., Jr., Anderson, C. F., & Lohman, T. M. (1978) *Q. Rev. Biophys. 11*, 103-178.
Saenger, W. (1984) *Principles of Nucleic Acids Structure*, Springer, Heidelberg.
Sampson, J. R., DiRenzo, A. B., Behlen, L. S., & Uhlenbeck, O. C. (1989) *Science 243*, 1363-1366.
Sanger, F., Nicklen, S., & Coulson, A. R. (1977) *Proc. Natl. Acad. Sci. U.S.A. 74*, 5463-5467.
Shippen-Lentz, D., & Blackburn, E. H. (1990) *Science 247*, 546-552.
Shore, D., Langowski, J., & Baldwin, R. L. (1981) *Proc. Natl. Acad. Sci. U.S.A. 78*, 4833-4837.
Symons, R. H. (1989) *Trends Biochem. Sci. (Pers. Ed.) 14*, 445-450.
Tang, R. S., & Draper, D. E. (1990) *Biochemistry 29*, 5232-5237.
Tirado, M. M., & Garcia de la Torre, J. (1979) *J. Chem. Phys. 71*, 2581-2587.
Uhlenbeck, O. C. (1987) *Nature 328*, 596-600.
Van den Hoogen, Y. T., van Beukezom, A. A., de Vroom, E., van der Marel, G. A., van Boom, J. H., & Altona, C. (1988) *Nucleic Acids Res. 16*, 5013-5030.
Varani, G., Wimberly, B., & Tinoco, I., Jr. (1989) *Biochemistry 28*, 7760-7772.
Westhof, E., Dumas, P., & Moras, D. (1985) *J. Mol. Biol. 184*, 119-145.
Wu, J.-M., & Crothers, D. M. (1984) *Nature 308*, 509-513.
Wu, H.-N., & Uhlenbeck, O. C. (1987) *Biochemistry 26*, 8221-8227.
Yamakawa, H., & Fuji, M. (1973) *Macromolecules 6*, 407-415.
Zaug, A. J., & Cech, T. R. (1986) *Science 231*, 470-475.
Zimm, B. H. (1980) *Macromolecules 13*, 592-602.

Interactions of Anilinoacridines with Nucleic Acids: Effects of Substituent Modifications on DNA-Binding Properties†

Randy M. Wadkins‡ and David E. Graves*
Department of Chemistry, University of Mississippi, University, Mississippi 38677
Received August 20, 1990; Revised Manuscript Received December 7, 1990

ABSTRACT: Spectroscopic methods are used to probe the interactions of several anilinoacridine analogues with calf thymus DNA over a wide range of temperatures and sodium chloride concentrations. The structurally similar compounds *m*-AMSA, AMSA (both active as antitumor agents), and *o*-AMSA (inactive as an antitumor agent) have been widely studied in their abilities to bind DNA in an intercalative manner. Recent studies from this laboratory reveal distinct differences in the thermodynamic binding mechanisms between *m*-AMSA and *o*-AMSA (Wadkins & Graves, 1989), with the *m*-AMSA–DNA interaction being an enthalpy-driven process while the binding of *o*-AMSA to DNA is characterized by more positive entropy values. To further examine the physical chemical properties associated with these compounds and their correlation with antitumor activities, an in-depth investigation into the thermodynamic parameters of these compounds and structurally related anilinoacridine analogues was performed. These studies demonstrate that substituent type and position on the aniline ring of the anilinoacridines greatly influences both the affinities of these drugs in binding to DNA and dictates whether the DNA binding is an enthalpy- or entropy-driven process. The differences in thermodynamic mechanisms of binding between the two isomers along with molecular modeling studies reveal the electronic and/or steric factors resulting from the positioning of the methoxy substituent group on the anilino ring directs the DNA-binding properties through orientation of the methanesulfonamido group at the 1′ position of the aniline ring. The orientation of this substituent group may result in favorable contacts through hydrogen bonding with neighboring base pairs and ultimately influence the biological effectiveness as an antitumor agent.

Amsacrine [4′-(9-acridinylamino)methanesulfon-*m*-anisidide, *m*-AMSA][1] is a 9-anilinoacridine analogue that was developed by Cain et al. (1975). This acridine analogue has been shown to be highly effective against experimental tumors and is particularly valuable because of its lower incidence of cardiotoxicity than the anthracyclines (Hall et al., 1983;

† This work was supported by a U.S. Public Health Service Research Grant, National Cancer Institute, CA-41474.
* Address correspondence to this author.
‡ Current address: Department of Molecular Biology, Max Planck Institute for Biophysical Chemistry, P.O. Box 2841, D-3400, Goettingen, FRG.

[1] Abbreviations: *m*-AMSA, 4′-(9-acridinylamino)methanesulfon-*m*-anisidide; *o*-AMSA, 4′-(9-acridinylamino)methanesulfon-*o*-anisidide; EDTA, ethylenediaminetetraacetic acid; bp, base pairs.

0006-2960/91/0430-4277$02.50/0